

# The evolution of the Čanište epidote-bearing pegmatite, Republic of Macedonia: evidence from mineralogical and geochemical features



Sabina Strmić Palinkaš<sup>1</sup>, Vladimir Bermanec<sup>1</sup>, Ladislav A. Palinkaš<sup>1</sup>, Blažo Boev<sup>2</sup>, Robert A. Gault<sup>3</sup>, Walter Prochaska<sup>4</sup>, Ronald J. Bakker<sup>4</sup>

<sup>1</sup> Institute of Mineralogy and Petrology, Department of Geology, Faculty of Science, University of Zagreb, Horvatovac 95, HR-10000 Zagreb, Croatia; (sabina.strmic@inet.hr)

<sup>2</sup> Faculty of Mining, Geology and Polytechnic, Goce Delčev University, Krste Misirkov bb, P.O. Box 201, MK-2000 Štip, Republic of Macedonia

<sup>3</sup> Research Division, Canadian Museum of Nature, P.O. Box 3443, Station D, Ottawa, Ontario K1P 6P4, Canada

<sup>4</sup> Department of Applied Geosciences and Geophysics, Mineralogy and Petrology Group, University of Leoben, Peter-Tunner-Strasse 5, A-8700 Leoben, Austria

doi: 104154/gc.2012.31

## Geologia Croatica

### ABSTRACT

The epidote-bearing Čanište pegmatite and adjacent Upper Carboniferous granodiorites cut Precambrian gneisses, on the western slopes of the Selečka Mts., the Eastern Pelagonian zone, Republic of Macedonia. The pegmatite exhibits zonal internal structure with the following sub-units: the wall zone (amazonite microcline ± biotite, quartz), the first intermediate zone (epidote + haematite + grossular + muscovite + quartz + almandine ± zircon, beryl, microcline, quartz), the second intermediate zone (albite + quartz ± microcline) and the core (massive quartz). According to the microprobe data epidote belongs to clinozoisite subgroup with the formula  $(Ca_{1.96-1.99}Mn_{0.02-0.03}Fe^{2+}_{0.00-0.02})(Al_{2.17-2.46}Fe^{3+}_{0.51-0.82}Ti_{0.00-0.01})(Si_2O_7)(Si_{0.99-1.00}Al_{0.00-0.01}O_4)O(OH)$ . The occurrences of almandine and zircon with low U, Th and REE content, are indicative of weakly evolved granitic/granodioritic rocks. The absence of aplites suggests steady pressure conditions during the course of pegmatite crystallization. Microthermometric data combined by the two-feldspar geothermometer gained pressure from 4.8 to 5.6 kbar for the second intermediate zone. The wall zone, composed of amazonite microcline, crystallized at a temperature between 650 and 760 °C. A drop in melt temperature to below 550 °C, under the oxygen fugacity between  $10^{-22}$  and  $10^{-19.5}$  bar, was the principal trigger for crystallization of minerals in the first intermediate zone. The residual fluid, depleted in Ca, Fe and K, and enriched in water, Na and Si, caused deposition of the second intermediate zone (albite + quartz) at temperatures between 445 and 465 °C. The massive quartz core crystallized in the very last stage of the pegmatite evolution ( $T \approx 400-480$  °C) from melt residue enriched in silica, water and CO<sub>2</sub> content.

**Keywords:** magmatic-hydrothermal transition, granodiorite, pegmatite, epidote, fluid inclusions, Pelagonian zone, Republic of Macedonia

### 1. INTRODUCTION

The Čanište pegmatite is situated approximately 150 km south of Skopje, Republic Macedonia, on the western slopes of the Selečka Mts. which represent a part of the Eastern

Pelagonian tectono-stratigraphic unit of the Dinaride-Hellenides (Fig. 1). The Pelagonian Massif exposes Precambrian crystalline basement made of ortho- and paragneisses, micaschists and amphibolites and comprises numerous pegmatites, which differ according to their size, mineralogical fea-

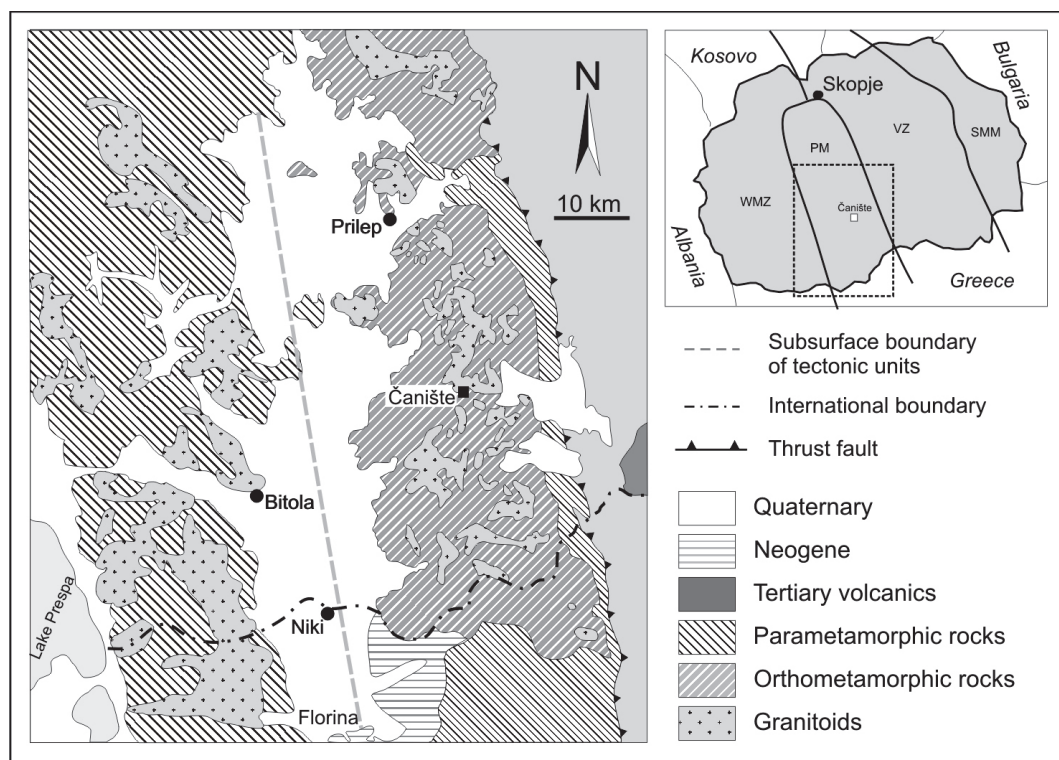


**Figure 1:** Geological setting of the Čanište epidote-bearing pegmatite, Republic of Macedonia (after MOST, 2003). WMZ – Western Macedonian zone; PM – Pelagonian massif; VZ – Vardar zone; SMM – Serbo-Macedonian massif.

tures, internal structures and the degree of fractionation (e.g. IVANOV et al., 1966; ZEBEC & RADANOVIĆ-GUŽVICA, 1992; JOVANOVSKI et al., 2003).

This pegmatite attracts attention due its peculiar Ca-enriched mineral assemblage with the unique occurrence of up to 2 metre long epidote crystals (BERMANEC et al., 2001). Epidote is not a common pegmatitic mineral and it has been recorded only within several epidote-bearing pegmatites elsewhere (e.g. FRANZ & SMELIK, 1995; JANEČEK, 2007; LIEBSCHER et al., 2007; COTA et al., 2010; SWANSON & VEAL, 2010). Furthermore, the Čanište pegmatite exhibits a zonal mineral distribution that allows a detailed investigation of fluid inclusions within minerals from the different stages of the pegmatite crystallization. Although the zonal pegmatites are common, and fluid inclusions rep-

resent relicts of fluids involved in the crystallization processes, only a few publications present the fluid inclusion data systematically collected across the distinct pegmatite zones (e.g. LONDON, 1986, 1990; THOMAS & SPOONER, 1988, 1992; FUERTES-FUENTE et al. 2000; BEURLIN et al., 2001; SIRBESCU et al., 2008).

The pegmatites are related to the late stage of magmatic crystallization. While the importance of volatiles and incompatible elements in enriched melts is generally accepted, there are still numerous open questions about the mechanism of their deposition. The majority of authors consider that water-saturated magmas are responsible for the principal mineralogical characteristics of pegmatites (e.g. JAHNS & BURNHAM, 1969; BURNHAM & NEKVASIL, 1986; NABELEK et al., 2010). In contrast, LONDON et al. (1989)

Sub-unit	The wall zone	The first intermediate zone	The second intermediate zone	The core
Mineral				
Microcline	—	—	—	—
Biotite	—	—	—	—
Quartz	—	—	—	—
Epidote	—	—	—	—
Muscovite	—	—	—	—
Hematite	—	—	—	—
Grossular	—	—	—	—
Almandine	—	—	—	—
Zircon	—	—	—	—
Beryl	—	—	—	—
Albite	—	—	—	—

**Figure 2:** Paragenetic sequence of the Čanište epidote-bearing pegmatite.

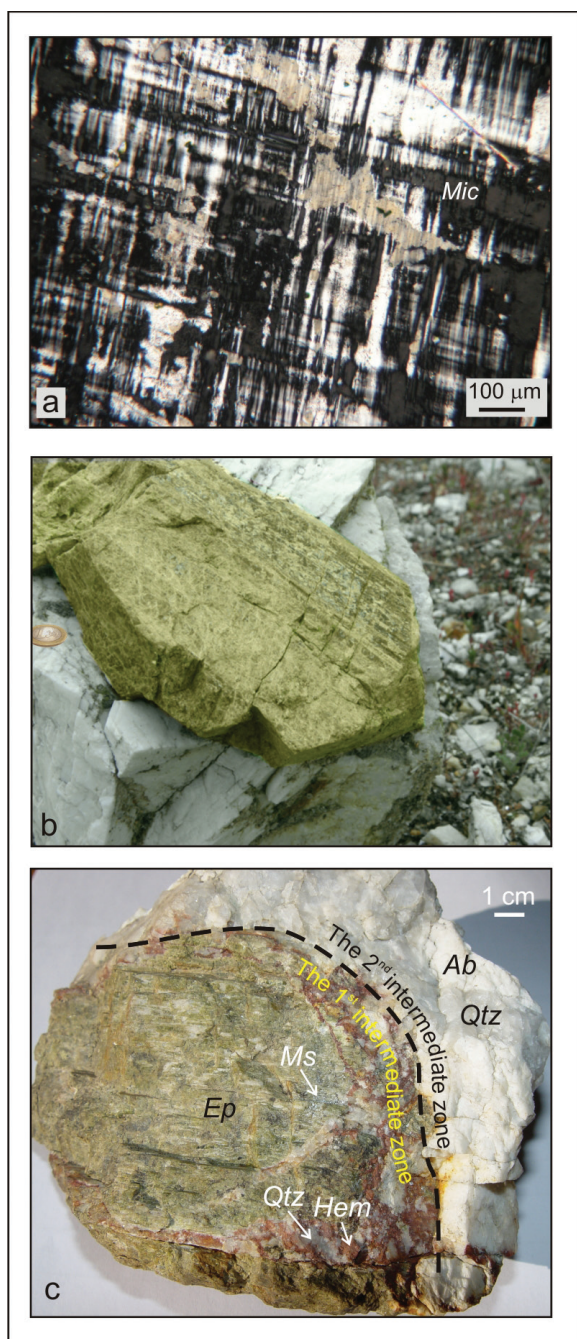


**Figure 3:** a) Photomicrographs of microcline from the wall zone; b) the transition from the first intermediate zone comprising epidote, hematite, muscovite and quartz into the second intermediate zone with albite and quartz. Abbreviations: Ab – albite; Ep – epidote; Hem – hematite; Mic – microcline; Ms – muscovite; Qtz – quartz.

and LONDON (1990, 2008) explain the formation of pegmatites by disequilibrium crystallization from water unsaturated magmas, emphasizing the role of fluxing elements such as B, F, and P.

The aim of this study is to interpret the evolution of melt-fluid in the late magmatic system responsible for deposition of the Čanište epidote-bearing pegmatite. A fluid inclusion study complemented by calculated thermodynamic equilibria of the mineral paragenesis shed light on the P-T-X conditions when the pegmatite formed.

## 2. GEOLOGICAL SETTING

The Pelagonian tectono-stratigraphic unit is a ca. 420 km long and 60 km broad in the NNW-SSE striking part of the central Hellenides (Fig. 1), exposing Precambrian crystalline basement made of ortho- and paragneisses, micaschists and amphibolites. Granitoids intruded the Pelagonian basement during: I) Upper Carboniferous and II) Late Permian – Early Triassic magmatic events (MOST, 2003). According to the QAP classification, Pelagonian granitoids range from granite to quartz-diorite, but are mainly granodioritic in composition (DUMURDZANOV, 1985; MOST, 2003). The Upper Carboniferous granodiorite ( $299 \pm 1$  Ma, U/Pb zircon age dating; MOST, 2003) underwent compressional deformation and developed a greenschist to amphibolite-grade metamorphic overprint. A Late Permian – Early Triassic granodiorite ( $\sim 245 \pm 1$  Ma, U/Pb zircon age dating; MOST, 2003) is represented by massive intrusive bodies within the Eastern Pelagonian zone, including the Selečka Mts. The relicts of concomitant metamorphism are not preserved. A sedimentary sequence, comprising carbonate and clastic rocks, was deposited during Triassic and Jurassic times. The geological structure of the Pelagonian zone is mostly a consequence of polyphase tectonometamorphic events during convergence of the Apulian and European plates between the Upper Jurassic and Upper Tertiary times (MOST, 2003).

The Čanište pegmatite is one of numerous pegmatite occurrences within the Eastern Pelagonian zone. The pegmatites vary in size from a few decimetres wide and tens of metres long to larger bodies tens of metres wide by hundreds of metres long. They differ according to the mineralogical features, the internal structures and the fractionation degree as well. Beside epidote-bearing ones (Čanište and Dunje localities), the most interesting are those enriched in uranium and thorium mineralization (Alinci and Crni Kamen localities; e.g. IVANOV et al., 1966; RADUSINOVIĆ & MARKOV, 1971; BERMANEC et al., 1988, 1992; ZEBEC & RADANOVIĆ-GUŽVICA, 1992).

The Čanište lens-shaped, up to 10 m wide pegmatite body, cuts Precambrian gneisses (DUMURDZANOV, 1985; MOST, 2003). The well developed internal zonation of the pegmatite is illustrated by an idealized paragenetic sequence (Fig. 2). Equigranular subhedral amazonite microcline is the main constituent of the wall zone (Fig. 3a), whereas quartz and biotite are accessory minerals. The first intermediate zone consists of giant epidote crystals (up to 2 m long; Fig. 3b), microcline, haematite, muscovite, garnet, quartz, and minor zircon and beryl (Fig. 3c). The second intermediate zone, composed of albite, quartz and minor microcline grades (Fig. 3c) into the monomineralic massive quartz core.

## 3. ANALYTICAL METHODS

Feldspar, epidote, quartz, garnet and zircon crystals were separated for X-ray powder diffraction (XRD) and electron-microprobe analyses. The XRD analyses were conducted on oriented samples using a Philips diffractometer PW 3040/60 X'Pert PRO (45 kV, 40  $\mu$ A) with  $\text{CuK}_\alpha$  monochromatised

**Table 1:** Representative microprobe analyses, calculated formulas and distribution of the key cation sites for epidote from the first intermediate zone of the Čanište epidote-bearing pegmatite.

	PT 1	PT 2	PT 3	PT 4	PT 5	PT 6	PT 7	PT 8	PT 9	
Chemical composition (wt. %)										
SiO <sub>2</sub>	36.82	36.74	37.36	36.86	36.79	36.88	37.45	37.07	37.66	
TiO <sub>2</sub>	< d.l.	0.09	< d.l.	0.08	< d.l.	< d.l.	0.09	0.07	0.12	
Al <sub>2</sub> O <sub>3</sub>	22.98	22.80	22.84	22.50	22.63	22.57	26.19	24.33	26.10	
Fe <sub>2</sub> O <sub>3</sub>	12.87	13.06	13.06	13.11	13.33	13.07	8.90	11.20	8.78	
MnO	0.44	0.41	0.44	0.55	0.49	0.49	0.25	0.36	0.25	
CaO	22.64	22.73	22.78	22.77	22.62	22.36	23.32	22.99	23.17	
H <sub>2</sub> O**	1.84	1.84	1.85	1.84	1.84	1.83	1.88	1.86	1.88	
TOT	97.59	97.67	98.33	97.71	97.70	97.20	98.08	97.88	97.96	
Structural formula (atom. %)										
Si <sup>4+</sup>	3.00	2.99	3.02	3.00	3.00	3.02	2.99	2.99	3.01	
Ti <sup>4+</sup>	0.00	0.01	0.00	0.00	0.00	0.00	0.01	0.00	0.01	
Al <sup>3+</sup>	2.21	2.19	2.18	2.16	2.17	2.18	2.46	2.31	2.46	
Fe <sup>3+</sup>	0.79	0.80	0.78	0.80	0.82	0.78	0.53	0.68	0.51	
Fe <sup>2+</sup>	0.00	0.00	0.02	0.00	0.00	0.02	0.00	0.00	0.02	
Mn <sup>2+</sup>	0.03	0.03	0.03	0.04	0.03	0.03	0.02	0.02	0.02	
Ca <sup>2+</sup>	1.98	1.98	1.97	1.99	1.98	1.96	1.99	1.99	1.98	
CATS	8.00	8.00	8.00	8.00	8.00	8.00	8.00	8.00	8.00	
Distribution of ions on key sites										
A1	Mn <sup>2+</sup>	0.03	0.03	0.03	0.04	0.03	0.03	0.02	0.02	0.02
	Fe <sup>2+</sup>	0.00	0.00	0.02	0.00	0.00	0.02	0.00	0.00	0.02
	Ca <sup>2+</sup>	0.97	0.97	0.95	0.96	0.97	0.94	0.98	0.98	0.97
A2	Ca <sup>2+</sup>	1.01	1.01	1.02	1.03	1.01	1.02	1.01	1.01	1.02
M1	Al <sup>3+</sup>	0.99	0.99	0.95	0.97	0.99	0.96	0.99	0.99	0.98
M2	Al <sup>3+</sup>	1.00	1.00	1.00	1.00	1.00	1.00	1.00	1.00	1.00
M3	Fe <sup>3+</sup>	0.79	0.80	0.78	0.80	0.82	0.78	0.53	0.68	0.51
	Ti <sup>4+</sup>	0.00	0.01	0.00	0.00	0.00	0.00	0.01	0.00	0.01
	Al <sup>3+</sup>	0.21	0.19	0.22	0.19	0.18	0.22	0.46	0.32	0.48
T	Si <sup>4+</sup>	3.00	2.99	3.02	3.00	3.00	3.02	2.99	2.99	3.01
	Al <sup>3+</sup>	0.00	0.01	0.00	0.00	0.00	0.00	0.01	0.01	0.00

< d.l. – below detection limit  
K, Na and Mg are below detection limits

\* Total iron content given as Fe<sub>2</sub>O<sub>3</sub>  
\*\* Determined by stoichiometry

radiation ( $\lambda=1.54056 \text{ \AA}$ ) and  $\theta$ - $\theta$  geometry. Samples were scanned between 4 and 63 ° 2 $\theta$  with 0.02 ° step per 0.5 minute. The goniometer was calibrated against a quartz standard. Phase identification was performed using X'Pert Highscore software package (PANalytical, 2004) in support with ICDD-PDF 2 database (2004). Unit cell parameters were calculated with the least-square refinement program UNIT-CELL (HOLLAND & REDFERN, 1997).

The chemical composition of selected samples was estimated by the JEOL 733 electron microprobe equipped with the Tracor Northern 5500 and 5600 automation. An accelerating voltage of 15 kV and a beam current of 20 nA were used in the analyses. Beam diameter varied with the mineral phase analyzed: 2  $\mu\text{m}$  for zircon, garnet and epidote and 20  $\mu\text{m}$  for

feldspars. The following standards were used: albite (Na, Al, Si), sanidine (K), gehlenite (Ca), almandine (Fe), rutile (Ti), tephroite (Mn), zircon (Zr), diopside (Mg), sanbornite (Ba), rubidium microcline (Rb), pollucite (Cs), crocoite (Pb), synthetic REE phosphates (La, Ce, Pr, Nd, Sm, Gd, Er, Yb), synthetic yttrium iron garnet (Y), synthetic hafnion (Hf), synthetic UO<sub>2</sub> (U) and synthetic ThO<sub>2</sub> (Th). Minimum detection limits for all analyzed range from 200 to 300 ppm.

Fluid inclusion investigations were carried out on microcline, albite, epidote and quartz crystals. Microthermometric measurements of fluid inclusions were performed using a Linkam THMS 600 stage mounted on an Olympus BX 51 microscope using 10x and 50x Olympus long-working distance objective lenses for visible light. Two synthetic fluid

inclusion standards (SYN FLINC; pure H<sub>2</sub>O and mixed H<sub>2</sub>O-CO<sub>2</sub>) were used to calibrate the equipment. The precision of the system was  $\pm 2.0$  °C for homogenization temperature, and  $\pm 0.2$  °C in the temperature range between  $-60$  and  $+10$  °C.

The laser Raman spectroscopy, used for the semiquantitative analysis of CO<sub>2</sub> and N<sub>2</sub> in the CO<sub>2</sub>-rich phases of fluid inclusions, was performed on the Dilor LabRAM instrument. A laser beam is focused through an Olympus BX 40 microscope onto the fluid inclusion of interest. The objective lenses of 50x and 100x magnification, combined with a confocal optical arrangement, enable a spatial resolution in the order of a cubic micrometer. Frequency-doubled Nd-YAG green laser (532 nm, 100 mV) was employed. Measurements can also be performed at temperature range between  $-190$  and  $600$  °C, using the Linkam THMSG 600 heating-cooling stage described above.

Bulk ion compositions of fluid inclusions were established by ion chromatographic analysis applying the technique modified after BOTTREL et al. (1988). About 1 g of cleaned grains and 5 ml of double-distilled and de-ionized water were ground with an agate mortar and pestle to fine powder. The milky solution produced was centrifuged to separate the leachate from the sample. A Dionex DX-500 system with a micromembrane suppressor and pulsed amperometric detector was used for analyses of anions and cations. Detection limits are in the 0.1 ppb ( $\mu\text{g/l}$ ) range.

### 3. RESULTS

#### 3.1. Mineralogy and chemical composition of minerals

The wall zone consists of amazonite microcline with the following unit cell characteristics  $a = 8.348(5)$  Å,  $b = 13.333(8)$  Å,  $c = 7.062(5)$  Å,  $\alpha = 91.15(7)^\circ$ ,  $\beta = 116.25(9)^\circ$ ,  $\gamma = 88.22(1)^\circ$  and  $V = 720.56(3)$  Å<sup>3</sup>. Minor biotite and quartz occur as well.

The first transitional zone represents mineralogically the most diverse unit of the Čanište pegmatite. It comprises euhedral columnar crystals of epidote, up to 2 m long, embedded in a medium- to coarse-grained matrix of haematite, muscovite, quartz, albite, microcline and garnet. Zircon and beryl grains occur sporadically.

The epidote lattice parameters, calculated on the basis of XRD patterns, ( $a = 8.890(2)$  Å,  $b = 5.634(2)$  Å,  $c = 10.147(2)$  Å,  $\beta = 115.40(2)^\circ$  and  $V = 459.1(2)$  Å<sup>3</sup>) correspond well to the data previously reported for epidote from other localities (e.g. BONAZZI & MENCHETTI, 1995). According to the electron-microprobe data (Table 1) and classification proposed by ARMBRUSTER et al. (2006), epidote from the Čanište pegmatite belongs to the clinozoisite subgroup with a general formula of Ca<sub>2</sub>Al<sub>2</sub>Fe<sup>3+</sup>(Si<sub>2</sub>O<sub>7</sub>)(SiO<sub>4</sub>)O(OH). The structural formula and the key cation sites calculated on the basis of  $\Sigma(A+M+T)=8$  are listed in Table 1.

Garnet crystals are not very common. They vary in size, reaching up to 2 cm and have a deep red color. The cell parameters, calculated from diffraction lines using the least-

**Table 2:** Representative microprobe analyses, calculated formulas, distribution of the key cation sites and the end-member contents for garnets from the first intermediate zone of the Čanište epidote-bearing pegmatite.

	PT 1	PT 2	PT 3	
Chemical composition (wt. %)				
SiO <sub>2</sub>	37.00	37.38	37.14	
TiO <sub>2</sub>	0.35	0.36	0.32	
Al <sub>2</sub> O <sub>3</sub>	20.07	20.18	19.97	
Fe <sub>2</sub> O <sub>3</sub>	1.65	1.56	1.71	
FeO	16.87	16.67	16.66	
MnO	6.91	6.57	6.70	
CaO	15.98	15.94	15.75	
MgO	0.27	0.29	0.30	
TOT	99.10	98.95	98.55	
Structural formula (atom. %)				
Si <sup>4+</sup>	2.97	3.00	2.99	
Ti <sup>4+</sup>	0.02	0.02	0.02	
Al <sup>3+</sup>	1.90	1.91	1.90	
Fe <sup>3+</sup>	0.10	0.09	0.10	
Fe <sup>2+</sup>	1.13	1.12	1.12	
Mn <sup>2+</sup>	0.47	0.45	0.46	
Ca <sup>2+</sup>	1.38	1.37	1.36	
Mg <sup>2+</sup>	0.03	0.04	0.04	
CATS	8.01	7.98	7.99	
O	12	12	12	
Distribution of ions on key sites				
X	Fe <sup>2+</sup>	1.12	1.12	1.13
	Mn <sup>2+</sup>	0.47	0.45	0.46
	Ca <sup>2+</sup>	1.38	1.37	1.37
	Mg <sup>2+</sup>	0.03	0.03	0.04
Y	Ti <sup>4+</sup>	0.02	0.02	0.02
	Al <sup>3+</sup>	1.87	1.88	1.88
	Fe <sup>3+</sup>	0.10	0.09	0.10
	Fe <sup>2+</sup>	0.01	0.00	0.00
Z	Si <sup>4+</sup>	2.97	3.00	2.99
	Al <sup>3+</sup>	0.03	0.00	0.01
The end-members content (mole %)				
Spessartine	15.9	15.2	15.5	
Pyrope	1.1	1.2	1.2	
Almandine	38.0	38.1	38.1	
Grossular	39.9	40.7	40.0	
Andradite	5.1	4.8	5.2	

squares method, are  $a = 11.713(2)$  Å and  $V = 1607(1)$  Å<sup>3</sup>. The molar proportions of garnet end-members were calculated from the electron microprobe data (Table 2) according to the procedure published by LOCOCK (2008). Grossular, with 39.9–40.7 mole %, represents the principal garnet con-

stituent. The proportion of almandine is estimated within a range between 38.0 and 38.1 mole %. Spessartine content spans between 15.2 and 15.9 mole %. Andradite and pyrope contents vary up to 5.2 and 1.2 mole %, respectively.

Pinkish, several cm long, zircon crystals display the following unit cell parameters:  $a = 6.811(4) \text{ \AA}$ ,  $b = 5.988(6) \text{ \AA}$  and  $V = 261.7(3) \text{ \AA}^3$ . Its chemical composition and structural formula, calculated on the basis of four atoms of oxygen per formula unit, are summarized in Table 3.

Albite and quartz represent the principal constituents of the second transitional zone. Amazonite microcline occurs sporadically. Blocky white albite occurs in the form of crystals up to 10 cm in size. The unit cell parameters, calculated from diffraction lines using the least-squares method, are  $a = 8.142(6) \text{ \AA}$ ,  $b = 12.784(3) \text{ \AA}$ ,  $c = 7.165(4) \text{ \AA}$ ,  $\alpha = 94.158(9)^\circ$ ;  $\beta = 94.158(9)^\circ$ ,  $\gamma = 87.741(0)^\circ$  and  $V = 665.0(9) \text{ \AA}^3$ . Amazonite microcline, locally intergrown with albite, displays the following unit cell characteristics  $a = 8.584(4) \text{ \AA}$ ,  $b = 12.980(6) \text{ \AA}$ ,  $c = 7.219(3) \text{ \AA}$ ,  $\alpha = 90.79(6)^\circ$ ,  $\beta = 115.96(3)^\circ$ ,  $\gamma = 87.60(4)^\circ$  and  $V = 721.5(4) \text{ \AA}^3$ . The chemical composition and structural formulae of feldspar from the second intermediate zone are reported in Table 4. The formulae were calculated on the basis of eight oxygen atoms per formula unit. The feldspars from the Čanište pegmatite are very homogeneous. The plagioclase composition averages about Ab-

**Table 3:** Representative microprobe analyses and calculated formulas for zircon from the first intermediate zone of the Čanište epidote-bearing pegmatite.

	Zircon		
	PT 1	PT 2	PT 3
Chemical composition (wt. %)			
ZrO <sub>2</sub>	64.73	64.83	64.93
HfO <sub>2</sub>	2.71	2.79	2.81
SiO <sub>2</sub>	32.36	32.50	32.46
TOT	99.80	100.12	100.20
Structural formula (atom. %)			
Zr <sup>4+</sup>	0.976	0.974	0.975
Hf <sup>4+</sup>	0.024	0.025	0.025
Si <sup>4+</sup>	1.000	1.001	1.000
CATS	2.000	2.000	2.000
O	4	4	4

Y, La, Ce, Pr, Nd, Sm, Gd, Er, Yb, Ti, Th and U are below detection limits.

$_{98}\text{An}_1\text{Or}_1$  with a total range of variation less than 1 mole% Ab. The alkali feldspar has compositions of  $\text{Ab}_6\text{Or}_{94}\text{An}_0$  with variation of less than 2 mole% Ab.



**Figure 4:** Photomicrographs of representative primary fluid inclusions from different sub-units of the Čanište epidote-bearing pegmatite: a) hydrosaline (L+V+S) inclusion recorded within microcline from the wall zone; b) two-phase (L+V) inclusion hosted by microcline from the wall zone; c) two-phase inclusion (L+V) within epidote from the first intermediate zone; d) three-phase inclusion (L+V+S) contains accidentally trapped anisotropic solid phase, epidote from the first intermediate zone; e) inclusion with accidentally trapped crystal, quartz from the second intermediate zone; f) two-phase (L+V) inclusions from the quartz core.

**Table 4:** Representative microprobe analyses and calculated formulas for feldspars from the second intermediate zone of the Čanište epidote-bearing pegmatite.

	Albite					Amazonite microcline			
	PT 1	PT 2	PT 3	PT 4	PT 5	PT 6	PT 7	PT 8	PT 9
Chemical composition (wt. %)									
Na <sub>2</sub> O	11.36	11.28	11.17	11.39	11.52	11.65	0.66	0.84	0.42
K <sub>2</sub> O	0.07	0.08	0.12	0.12	0.07	0.13	15.62	15.25	15.79
Rb <sub>2</sub> O	< d.l.	0.22	0.25	0.11					
Cs <sub>2</sub> O	< d.l.	0.07	0.06	< d.l.					
CaO	0.31	0.29	0.72	0.21	0.15	0.14	< d.l.	< d.l.	< d.l.
BaO	< d.l.	< d.l.	< d.l.	0.57					
PbO	< d.l.	0.34	0.41	0.14					
Al <sub>2</sub> O <sub>3</sub>	20.08	19.93	20.52	19.63	19.81	19.68	18.25	18.38	18.61
Fe <sub>2</sub> O <sub>3</sub>	< d.l.	< d.l.	0.06	0.06	0.06	0.06	< d.l.	< d.l.	< d.l.
SiO <sub>2</sub>	68.91	68.87	68.12	69.31	69.52	69.23	65.24	64.54	64.47
TOT	100.73	100.45	100.71	100.72	101.13	100.89	100.40	99.73	100.11
Structural formula (atom. %)									
Na <sup>+</sup>	0.954	0.949	0.940	0.956	0.963	0.978	0.059	0.075	0.038
K <sup>+</sup>	0.004	0.005	0.007	0.007	0.004	0.007	0.919	0.903	0.934
Rb <sup>+</sup>	0.000	0.000	0.000	0.000	0.000	0.000	0.007	0.007	0.003
Cs <sup>+</sup>	0.000	0.000	0.000	0.000	0.000	0.000	0.001	0.001	0.000
Ca <sup>2+</sup>	0.015	0.013	0.034	0.010	0.007	0.006	0.000	0.000	0.000
Ba <sup>2+</sup>	0.000	0.000	0.000	0.000	0.000	0.000	0.000	0.000	0.010
Pb <sup>2+</sup>	0.000	0.000	0.000	0.000	0.000	0.000	0.004	0.005	0.002
Al <sup>3+</sup>	1.025	1.020	1.050	1.002	1.007	1.004	0.992	1.006	1.016
Fe <sup>3+</sup>	0.000	0.000	0.002	0.002	0.002	0.002	0.000	0.000	0.000
Si <sup>4+</sup>	2.985	2.990	2.958	3.001	2.998	2.996	3.008	2.996	2.988
CATS	4.982	4.977	4.990	4.978	4.981	4.993	4.989	4.994	4.991
O	8	8	8	8	8	8	8	8	8

&lt; d.l. – below detection limit

Sr, Mn and P are below detection limits.

The partitioning of the albite component between coexisting microcline and plagioclase solid-solutions can be employed as a pressure-dependent geothermometer (WHITNEY & STROMER, 1977). Whereas temperature estimated from the two-feldspar geothermometer increases with pressure by 18 °C per kilobar (STROMER & WHITNEY, 1985), the formation temperature can be determined through a combination of the two-feldspar geothermometer with the fluid inclusion data (Fig. 6).

### 3.2. Fluid inclusion studies

Fluid inclusions from the wall zone amazonite microcline were classified as either primary or secondary according to

the criteria proposed by ROEDDER (1984). Primary fluid inclusions are sub-rounded to irregular in shape and up to 10 µm in size. Usually these inclusions occur in individual clusters or in isolation. Based on the number of phases, the primary microcline-hosted fluid inclusions could be subdivided into two additional sets: 1) polyphase (L+V+S) and 2) two-phase (L+V) inclusions.

Polyphase inclusions comprise up to 50 vol. % of solid phases, highly saline aqueous solution and vapour bubbles (Fig. 4a). Solid phases are usually transparent and inactive in Raman spectra. Salt melting temperatures from 450 °C up to 600 °C (the limit of the heating-freezing stage) suggest salinity higher than 53.3 wt. % NaCl equ. (BODNAR & VITYK, 1994). According to Raman microspectroscopy data the vapour bubbles contain only water vapour. Total homogenization occurs by the vapour phase disappearance at temperatures higher than 480 °C. The part of fluid inclusions did not homogenize below the upper temperature limit of the heating stage (600 °C), and consequently the bulk fluid properties and isochores can be calculated only for those inclusions with total homogenization below 600 °C (Fig. 6).

Two phase inclusions contain liquid and vapour phases at room temperature (Fig. 4b). Degree of fill (F) varies between 0.75 and 0.80. Eutectic temperature ( $T_e$ ) around –52

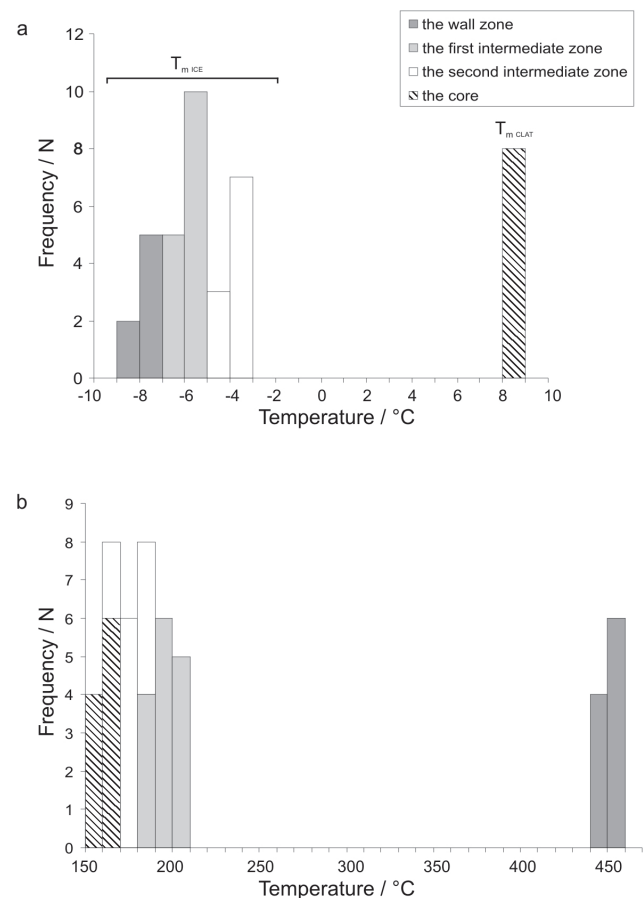


**Figure 5:** Microthermometric data for fluid inclusions from different sub-units of the Čanište epidote-bearing pegmatite; a) Plots of ice-melting ( $T_{m\text{ICE}}$ ) and clathrate-melting ( $T_{m\text{CLAT}}$ ) temperatures; b) Plots of homogenization temperatures.

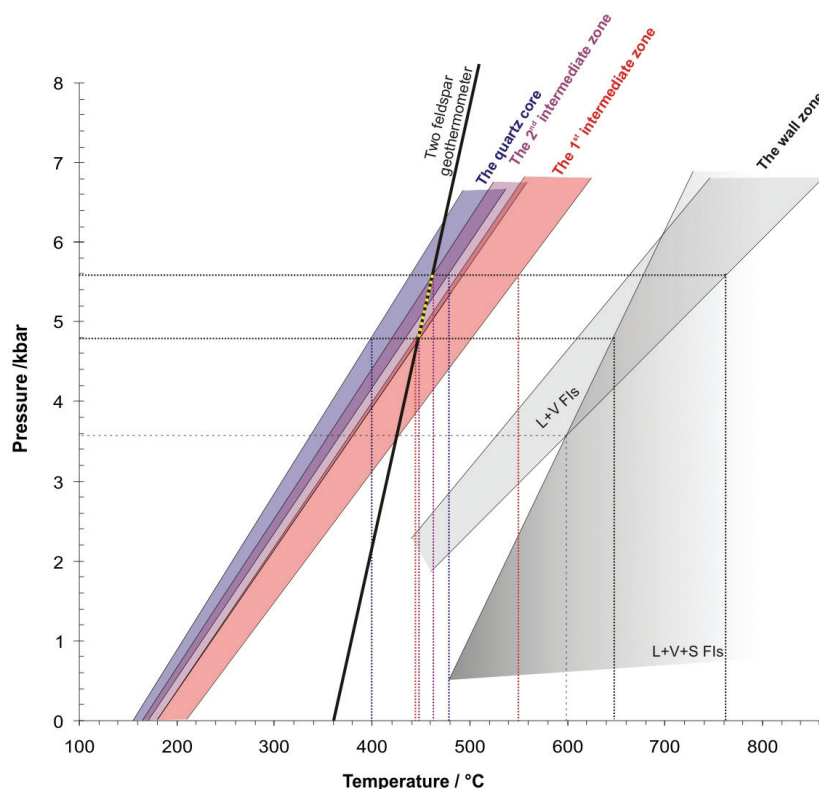


**Figure 6:** Pressure–temperature diagram summarizing the relevant information relating to the P–T history of the Čanište epidote-bearing pegmatite.

°C suggests  $\text{CaCl}_2$  and  $\text{NaCl}$  as the dominant dissolved salts (CRAWFORD, 1981). The final ice melting temperature ( $T_{m, \text{ICE}}$ ) has been measured between  $-7.5$  and  $-8.5$  °C (Fig. 5a). The final ice melting temperatures and experimental data published by BODNAR (1993) for the system  $\text{H}_2\text{O}-\text{NaCl}$ , indicate salinity ranges from 11.1 to 12.3 wt.%  $\text{NaCl}$  equ. Total homogenization ( $T_H$ ) occurs between 440 and 460 °C by vapour-bubble disappearance (Fig. 5b). Bulk fluid density, utilizing the equation of state proposed by ARCHER (1992) through the BULK software (BAKKER, 2003), spans from 0.809 to 0.863  $\text{g}/\text{cm}^3$ . The isochores were calculated with the ISOC software (BAKKER, 2003) utilizing the equations of BOWERS & HELGESON (1983) and BAKKER (1999) (Fig. 6).

The secondary inclusions in the wall zone amazonite microcline lie along curved trails, display irregular shape and comprise two phases (L+V). Their size below 5  $\mu\text{m}$  precludes microthermometric measurements.

Epidote is the only mineral from the first intermediate zone that hosts fluid inclusions large enough for microthermometric measurements. Primary fluid inclusions occur either isolated or as clusters. They are two-phase (liquid + vapour) up to 15  $\mu\text{m}$  in size, with an elongated, rounded or irregular shape (Fig. 4c). Some inclusions enclose birefringent insoluble solids (Fig. 4d). The solids might be crystals trapped accidentally during the formation of fluid inclusions, rather than daughter minerals, judging by their inconsistent phase ratios. The vapour phase occupies around 20% of the total volume. Raman microspectroscopy only revealed the presence of water.

Initial melting temperature between  $-42$  and  $-62$  °C suggests the presence of divalent cations, most likely Ca, Fe and Mg (BARKER, 1995). The final ice melting temperature spanning from  $-5.6$  to  $-6.7$  °C (Fig. 5a) indicates moderately saline fluids (8.7 and 10.1 wt.%  $\text{NaCl}$  equ.). Homogenization to a liquid phase occurs at temperatures between 180 and 210 °C (Fig. 5b). The calculated fluid density ranges from 0.925 to 0.961  $\text{g}/\text{cm}^3$ .

The bulk leachate data of fluid inclusions in epidote suggest  $\text{Cl}^-$  as major anion and  $\text{Na}^+$  and  $\text{Mg}^{2+}$  as the dominant cations (Table 5).

Secondary inclusions, distributed along healed fractures of random orientation, were too small for microthermometric measurements (less than 5  $\mu\text{m}$ ).

Fluid inclusions were examined in quartz and albite from the second intermediate zone. The majority of the inclusions have a size below 10  $\mu\text{m}$ . Primary inclusions occur as single, isolated inclusions, or as randomly oriented groups, and commonly mark zones of host crystal growth. These inclusions exhibit irregular to rounded shapes and contain liquid and vapour phases with consistent volumetric proportions ( $F \approx 0.80$ ). Frequently, inclusions comprise an insoluble solid phase, interpreted as accidentally trapped crystals (Fig. 4e). Raman microspectroscopy recorded only the presence of water, as for the samples from the first intermediate zone.

Eutectic temperatures around  $-52$  °C indicate a Ca–Na–Cl system (SHEPHERD et al., 1985). The temperatures of final ice melting ranging from  $-3.4$  to  $-4.2$  °C (Fig. 5a) corresponding to salinity between 5.6 and 6.7 wt.%  $\text{NaCl}$  equ. Temperatures of homogenization into a liquid phase were recorded within an interval between 165 and 180 °C (Fig.

5b). Bulk fluid density, estimated from fluid inclusion data, spans from 0.931 to 0.951 g/cm<sup>3</sup>. Constructed isochores are shown in Figure 6. The intersection of isochores with the two-feldspar geothermometer published by WHITNEY & STROMER (1977), and corrected for pressure according to the procedure described by STROMER & WHITNEY (1985), revealed the formation temperature of the second intermediate zone in the range between 445 and 465 °C under pressure between 4.8 and 5.6 kbar.

Fluid inclusions from the monomineralic massive quartz core show irregular to rounded shapes and range in size up to 15 μm (Fig. 4f). They occur either isolated or in clusters of 5 to 10 inclusions arranged in three-dimensional, non-planar arrays. Inclusions comprise two phases (liquid and vapour) and have uniform degree of fill around 0.8. Micro-Raman spectroscopy measurements recognized the presence of CO<sub>2</sub> within the vapour phase.

Due to poor optical quality, an initial melting temperature (eutectic temperature, T<sub>e</sub>) was not detected. The formation of the CO<sub>2</sub> clathrate phase additionally hampers interpretation of low temperature microthermometric data. Clathrate melting temperature (T<sub>m CLAT</sub>) in the interval between +8.1 and +8.9 °C (Fig. 5a) corresponds to a salinity of 2.2 to 3.8 wt.% equ. NaCl. Homogenization of the carbonic phase proceeds into vapour phase around 28 °C. Total homogenization by vapour-bubble disappearance occurs in a temperature range between 155 and 170 °C (Fig. 5b). Bulk fluid density, calculated by the BULK software (BAKKER, 2003), ranges between 0.882 and 0.892 g/cm<sup>3</sup>.

The leachate data revealed the predominance of Na<sup>+</sup>, K<sup>+</sup> and Cl<sup>-</sup> in the aqueous fluids responsible for the massive quartz core crystallization (Table 5).

#### 4. DISCUSSION

Magmatic differentiation by crystal fractionation generally results in the transition of low-volatile content silicate melt (producing normal igneous rocks), through hydrous silicate melt (producing pegmatites), to late-stage water-rich fluids (producing metal ore deposits) (ROEDDER, 1992). The majority of fluid inclusion studies performed on pegmatites suggest crystallization from a water-saturated system and, consequently, immiscibility between the melt phase and volatile fluid (e.g. BEURLEN et al., 2001; THOMAS et al., 2011; THOMAS & DAVIDSON, 2012).

The crystallization evolution of the Čanište epidote-bearing pegmatite, is reconstructed using thermodynamic mineral equilibria and fluid inclusion data. The pegmatite

originates from intrusion of granodioritic melt into the Pelagonian crystalline basement in the Upper Carboniferous (MOST, 2003). The melt that ultimately produced the Čanište pegmatite was relatively Fe-rich in its initial stage, as indicated by the crystallization of epidote, haematite and almandine. The complete absence of fluxes (B, P, F), and relatively high concentrations of compatible elements (e.g., Ca, Fe, Zr) are very different in comparison to common granitic systems, although similar chemistry has been related with leucotonalitic to quartz leucogabbroic pegmatites (NOVÁK & GADAS, 2010). The Čanište pegmatite exhibits a zoned internal structure with four distinctive zones: the wall zone, two intermediate zones and the quartz core. Textural characteristics suggest primary crystallization from melt in order; wall zone → first intermediate zone → second intermediate zone → core. The progressive crystallization resulted in melt composition changes. Concentrations of Ca, Fe and K decreased, and concentrations of Na and Si increased. Fluid inclusion data suggest subsequent crystallization under a steady decrease of temperature and isobaric conditions. Furthermore, fluid inclusion study indicates that aqueous fluids played an important role in the genesis of the Čanište pegmatite. The CO<sub>2</sub> content increased with progressive fractional crystallization, and a significant amount of CO<sub>2</sub> is present only in the very late stage of crystallization.

The presence of primary highly saline aqueous inclusions in the wall zone microcline supports the magmatic origin of the entrapped fluid (e.g. ROEDDER, 1992). Coexisting polyphase (L+V+S) and two-phase (L+V) inclusions as well as large variation in salinity suggest the accidental entrapment near the L/L+S interface of the P-T-X space (e.g. BAKKER & ELBURG, 2006). Whereas the trapping conditions might be estimated from the intersection of isochores constructed for two sets of simultaneously trapped fluid inclusions, and assuming that two principal sets of primary inclusions are contemporaneous, only the minimum possible formation temperature and pressure (600 °C, 3.8 kbar; Fig. 6) can be defined due to lack of homogenization temperatures for high temperature polyphase inclusions. The absence of aplites indicates a nearly constant pressure during pegmatite crystallization (e.g. NABELEK et al., 2010). Assuming a pressure of between 4.8 and 5.6 kbar, (estimated for the second intermediate zone by the combination of two-feldspar geothermometer and fluid inclusion data), the formation temperature of the wall zone then ranges from ca. 650 to 760 °C (Fig. 6).

The formation temperature of the first intermediate zone in the interval between 445 and 550 °C is constrained from the microthermometric data obtained on epidote, assuming

**Table 5:** The bulk leachate analyses for epidote and quartz from the Čanište epidote-bearing pegmatite.

Sample	Sub-unit	Li <sup>+</sup>	Na <sup>+</sup>	K <sup>+</sup>	Mg <sup>2+</sup>	Ca <sup>2+</sup>	F <sup>-</sup>	Cl <sup>-</sup>	Br	I <sup>-</sup>	NO <sub>3</sub> <sup>-</sup>	SO <sub>4</sub> <sup>2-</sup>	a <sub>Na<sup>+</sup>}/a<sub>K<sup>+</sup></sub></sub>	a <sub>Na<sup>+</sup>}/a<sub>Ca<sup>2+</sup></sub></sub>
		μmol/L												
Epidote	The 1 <sup>st</sup> intermediate zone	3.50	75.9	40.0	61.5	0.02	14.1	148.7	0.2	0.00	2.1	2.0	2	230787
Quartz	The quartz core	0.70	32.4	12.0	0.0	5.68	12.2	22.2	0.0	0.01	4.0	2.2	3	185



Na-enriched melt. The formation temperature estimated from the fluid inclusion data, as well as from two-feldspar geothermometer, spans the range from 445 to 465 °C. The massive quartz core was produced at temperatures between 400 and 480 °C from the very last melt residue enriched in silica, water and CO<sub>2</sub> content.

## ACKNOWLEDGMENT

We are grateful to reviewers, Pavel UHER and Sibila BOROJEVIĆ ŠOŠTARIĆ, whose comments significantly improved the paper. This study was supported by the Croatian Ministry of Sciences, Technology and Sports (Projects No. 119-0982709-1175 and No. 119-0000000-1158).

## REFERENCES

- ANOVITZ, L.M., ESSENE, E.J., METZ, G.W., BOHLEN, S.R., WESTRUM, E.F. JR. & HEMINGWAY, B.S. (1993): Heat capacity and phase equilibria of almandine, Fe<sub>3</sub>Al<sub>2</sub>Si<sub>3</sub>O<sub>12</sub>.—*Geochim. Cosmochim. Acta*, 57, 4191–4204. doi: 10.1016/0016-7037(93)90315-N
- ARCHER, D.G. (1992): Thermodynamic properties of the NaCl+H<sub>2</sub>O System. II. Thermodynamic properties of NaCl (aq), NaCl•2H<sub>2</sub>O(cr) and phase equilibria.—*J. Phys. Chem. Ref. Data*, 21, 793–829. doi:10.1063/1.555915
- ARMBRUSTER, T., BONAZZI, P., AKASAKA, M., BERMANEC, V., CHOPIN, C., GIERÉ, R., HEUSS-ASSBICHLER, S., LIEBSCHER, A., MENCHETTI, S., PAN, Y. & PASERO, M. (2006): Recommended nomenclature of epidote-group minerals.—*Eur. J. Mineral.*, 18, 551–567. doi: 10.1127/0935-1221/2006/0018-0551
- BAKKER, R.J. (1999): Adaption of Bowers & Helgeson (1983) equation of state to isochore and fugacity coefficient calculation in the H<sub>2</sub>O-CO<sub>2</sub>-CH<sub>4</sub>-N<sub>2</sub>-NaCl fluid system.—*Chem. Geol.*, 154, 225–236. doi: 10.1016/S0009-2541(98)00133-8
- BAKKER, R.J. (2003): Package FLUIDS 1. Computer programs for analysis of fluid inclusion data and for modelling bulk fluid properties.—*Chem. Geol.*, 194, 3–23. doi: 10.1016/S0009-2541(02)00268-1
- BARKER, A.J. (1995): Post-entrapment modification of fluid inclusions due to overpressure: evidence from natural samples.—*J. Metamorph. Geol.*, 13, 737–750. doi: 10.1111/j.1525-1314.1995.tb00256.x
- BERMANEC, V., TIBLJAŠ, D., GESSNER, M. & KNIEWALD, G. (1988): Monazite in hydrothermal veins from Alinci, Yugoslavia.—*Mineral. Petrol.*, 38, 139–150. doi: 10.1007/BF01164318
- BERMANEC, V., TIBLJAŠ, D. & KNIEWALD, G. (1992): Uranium-rich metamict senaite from Alinci, Macedonia, Yugoslavia.—*Eur. J. Mineral.*, 4, 331–335.
- BERMANEC, V., PALINKAŠ, L.A. & STRMIĆ, S. (2001): Mineralogy of pegmatite with giant epidote crystals, near Čanište, Macedonia.—In: PIESTRZYŃSKI, A. (ed.): *Mineral Deposits at the Beginning of the 21st Century*, Proceed. 6th biennial SGA meeting, 939–942.
- BEURLEN, H., DA SILVA, M.R.R., DE CASTRO, C. (2001): Fluid inclusion microthermometry in Be-Ta-(Li-Sn)-bearing pegmatites from the Borborema Province, Northeast Brazil.—*Chem. Geol.*, 173, 107–123. doi: 10.1016/S0009-2541(00)00270-9
- BODNAR, R.J. (1993): Revised equation and table for determining the freezing point depression of H<sub>2</sub>O-NaCl solutions.—*Geochim. Cosmochim. Acta*, 57, 683–684. doi: 10.1016/0016-7037(93)90378-A
- BODNAR, R.J. & VITYK M.O. (1994): Interpretation of microthermometric data for H<sub>2</sub>O-NaCl fluid inclusions. In: DE VIVO, B. & FREZZOTTI M.L. (Eds.): *Fluid Inclusions in Minerals, Methods and Applications*, Virginia Tech, Blacksburg, VA, 117–130.
- BONAZZI, P. & MENCHETTI, S. (1995): Monoclinic members of the epidote group: effects of the Al, Fe<sup>3+</sup>, Fe<sup>2+</sup> substitution and of the entry of REE<sup>3+</sup>.—*Mineral. Petrol.*, 53, 133–153. doi: 10.1007/BF01171952
- BOTTRELL, S.H., YARDLEY, B.W.D. & BUCKLEY, F. (1988): A modified crush-leach method for analysis of fluid inclusion electrolytes.—*Bull. Mineral.*, 111, 279–290.
- BOWERS, T.S. & HELGESON, H.C. (1983): Calculation of the thermodynamic and geochemical consequences of nonideal mixing in the system H<sub>2</sub>O-CO<sub>2</sub>-NaCl on phase relations in geological systems: equation of state for H<sub>2</sub>O-CO<sub>2</sub>-NaCl fluids at high pressures and temperatures.—*Geochim. Cosmochim. Acta*, 47, 1247–1275. doi: 10.1016/0016-7037(83)90066-2
- BUMHAM, C.W. & NEKVASIL, H. (1986): Equilibrium properties of granite pegmatite magmas.—*Am. Min.*, 71, 239–263.
- CAN, I. (2002): A new improved Na/K geothermometer by artificial neural networks.—*Geothermics*, 31, 751–760. doi: 10.1016/S0375-6505(02)00044-5
- COTA, A.C., WISE, M.A. & OWENS, B.E. (2010): Textural and chemical constraints on the origin of epidote in granitic pegmatites.—*Geol. Soc. Am., Abstracts with Progr.*, 42, p. 159.
- CRAWFORD, M.L. (1981): Phase equilibria in aqueous fluid inclusions.—*Mineral. Assoc. Can., Short Course*, 6, 75–100.
- DUMURDZANOV, N. (1985): Petrogenetic characteristics of the high metamorphic and magmatic rocks of the Central and Western part of the Selečka Mts. (Pelagonian massif), SR Macedonia, Yugoslavia.—*Geol. Maced.*, 2, 173–220.
- FRANZ, G. & SMELIK, E.A. (1995): Zoisite-clinozoisite bearing pegmatites and their importance for decompressional melting in eclogites.—*Eur. J. Mineral.*, 7, 1421–1436.
- FUERTES-FUENTE, M., AGUSTIN, M.-I., BOIRON, M.C. & VINUELA, J.M. (2000): P-T path and fluid evolution in the Franqueira granitic pegmatite, Central Galicia, northwestern Spain.—*Can. Min.*, 38, 1163–1175. doi: 10.2113/gscanmin.38.5.1163
- HELGESON, H.C., DELANY, J.M., NESBITT, H.W. & BIRD, D.K. (1978): Summary and critique of the thermodynamic properties of rock-forming minerals.—*Am. J. Sci.*, 278-A, 1–229.
- HOLLAND, T.J.B. & REDFERN, S.A.T. (1997): Unit cell refinement from powder diffraction data: The use of regression diagnostics.—*Mineral. Mag.*, 61, 65–77.
- ICDD POWDER DIFFRACTION FILE 2 (2004): Database Sets 1–54. International Centre for Diffraction Data (ICDD), Newton Square, Pennsylvania, USA.
- IVANOV, T., BOGOEVSKI, K., RADOVIĆ, N. & IVANOVA, V. (1966): Guidebook for Fieldtrips in SR Macedonia, Yugoslavia.—6th Meeting of Geologists of Yugoslavia, Ohrid, 17 p.
- JAHNS, R.H. & BURNHAM, C.W. (1969): Experimental studies of pegmatite genesis: I. A model for the derivation and crystallization of granitic pegmatites.—*Econ. Geol.*, 64, 843–864. doi: 10.2113/gsecongeo.64.8.843
- JANECZEK, J. (2007): Intragranitic pegmatites of the Strzegom-Sobótka massif – an overview.—In: KOZOWSKI, A. & WISZNIĘWSKA, J. (eds.): *Granitoids in Poland*. Arch. Miner. Monogr., 1, 193–201.
- JOVANOVSKI, G., BOEV, B., MAKRESKI, P., NAJDOSKI, M. & MLADENOVSKI, G. (2003): Minerals from Macedonia. XI. Silicate varieties and their localities – identification by FT IR spectroscopy.—*Bull. Chem. Technol. Macedonia*, 22, 111–141.
- KELLEY, K.K. (1960): Contributions to the data in theoretical metallurgy XIII: High temperature heat content, heat capacities and entropy data for the elements and inorganic compounds.—*U. S. Bureau of Mines Bulletin*, 584, 1–232.

- LIEBSCHER, A., FRANZ, G., FREI, D. & DULSKI, P. (2007): High-pressure melting of eclogite and the P–T–X history of tonalitic to trondhjemitic zoisite-pegmatites, Münchberg Massif, Germany.– *J. Petrology*, 48, 1001–1019. doi: 10.1093/petrology/egm008
- LOCOCK, A.J. (2008): An Excel spreadsheet to recast analyses of garnet into end-member components, and a synopsis of the crystal chemistry of natural silicate garnets.– *Comput. & Geosci.*, 34, 1769–1780. doi: 10.1016/j.cageo.2007.12.013
- LONDON, D. (1986): Magmatic-hydrothermal transition in the Tanco rare-element pegmatite; evidence from fluid inclusions and phase-equilibrium experiments.– *Am. Min.*, 71, 76–395.
- LONDON, D. (1990): Internal differentiation of rare-element pegmatites: a synthesis of recent research.– *Geol. Soc. Am., Spec. Pap.*, 246, 35–50.
- LONDON, D., MORGAN, G.B. & HERVIG, R.L. (1989): Vapor-undersaturated experiments in the system macusanite-H<sub>2</sub>O at 200 MPa, and the internal differentiation of granitic pegmatites.– *Contrib. Mineral. Petrol.*, 102, 1–17. doi: 10.1007/BF01160186
- MOST, T. (2003): Geodynamic evolution of the Eastern Pelagonian zone in Northwestern Greece and the Republic of Macedonia.– Unpubl. PhD Thesis, University of Tuebingen, Tuebingen, 195 p.
- NABELEK, P.I., WHITTINGTON, A.G. & SIRBESCU, M.-L.C. (2010): The role of H<sub>2</sub>O in rapid emplacement and crystallization of granite pegmatites: resolving the paradox of large crystals in highly undercooled melts.– *Contrib. Mineral. Petrol.*, 160, 313–325. doi: 10.1007/s00410-009-0479-1
- NOVAK, M. & GADAS, P. (2010): Zoned, anorthite- and grossularite-bearing, leucotonalitic pegmatite from serpentinized lherzolite at Ruda Nad Moravou, Staré Město Unit, Czech Republic.– *Can. Min.*, 48, 629–650. doi: 10.3749/canmin.48.3.629
- PANALYTICAL (2004): X'Pert Highscore Plus version 2.1. PANalytical, Almelo, Netherlands.
- RADUSINOVIĆ, D. & MARKOV C. (1971): Macedonite - lead titanate: a new mineral.– *Am. Min.*, 56, 387–394.
- ROEDDER, E. (1992): Fluid inclusion evidence for immiscibility in magmatic differentiation.– *Geochim. Cosmochim. Acta*, 56, 5–20. doi: 10.1016/0016-7037(92)90113-W
- SCHMIDT, M.W. & POLI, S. (2004): Magmatic epidote.– *Rev. Min. Geochem.*, 56, 399–430. doi: 10.2138/gsrmg.56.1.399
- SHEPHERD, T.J., RANKIN, A.H. & ALDERTON, D.H.M. (1985): A practical guide to fluid inclusion studies. Blackie, Glasgow, 239 p.
- SHOCK, E.L. & HELGESON, H.C. (1988): Calculation of the thermodynamic and transport properties of aqueous species at high pressures and temperatures: Correlation algorithms for ionic species and equation of state predictions to 5 kb and 1000°C.– *Geochim. Cosmochim. Acta*, 52, 2009–2036. doi: 10.1016/0016-7037(88)90181-0
- SIRBESCU, M.-L.C., HARTWICK, E.E. & STUDENT, J.J. (2008): Rapid crystallization of the Animikie Red Ace Pegmatite, Florence county, northeastern Wisconsin: Inclusion microthermometry and conductive-cooling modelling.– *Contrib. Mineral. Petrol.*, 156, 289–305. doi: 10.1007/s00410-008-0286-0
- SWANSON, S.E. & VEAL, W.B. (2010): Mineralogy and petrogenesis of pegmatites in the Spruce Pine District, North Carolina, USA.– *J. Geosciences*, 55, 27–42. doi: 10.3190/jgeosci.062
- THOMAS, A.V. & SPOONER E.T.C. (1988): Fluid inclusions in the system H<sub>2</sub>O-CH<sub>4</sub>-NaCl-CO<sub>2</sub> from metasomatic tourmaline within the border unit of the Tanco zoned granitic pegmatite, S.E. Manitoba.– *Geochim. Cosmochim. Acta*, 52, 1065–1075. doi: 10.1016/0016-7037(88)90261-X
- THOMAS, A.V. & SPOONER E.T.C. (1992): The volatile geochemistry of magmatic H<sub>2</sub>O-CO<sub>2</sub> fluid inclusions from the Tanco zoned granitic pegmatite, southeastern Manitoba, Canada.– *Geochim. Cosmochim. Acta*, 56, 49–65. doi: 10.1016/0016-7037(92)90116-Z
- THOMAS, R., DAVIDSON P., BEURLEN, H. (2011): Tantalite-(Mn) from the Borborema Pegmatite Province, northeastern Brazil: conditions of formation and melt- and fluid-inclusion constraints on experimental studies.– *Miner. Deposita*, 46, 749–759. doi: 10.1007/s00126-011-0344-9
- THOMAS, R. & DAVIDSON P. (2012): Water in granite and pegmatite-forming melts.– *Ore Geol. Rev.*, 46, 32–46. doi: 10.1016/j.oregeorev.2012.02.006
- TULLOCH, A.J. (1986): Comment on “Implications of magmatic epidote-bearing plutons on crustal evolution in the accreted terranes of northwestern North America” and “Magmatic epidote and its petrologic significance”.– *Geology*, 14, 187–188. doi: 10.1130/0091-7613(1986)14<186:CAROIO>2.0.CO;2
- WAGMAN, D. D., EVANS, W.H., PARKER, V.B., SCHUMM, R.H. & HALOW, I. (1982): The NBS tables of chemical thermodynamic properties. Selected values for inorganic and C1 and C2 organic substances in SI units.– *J. Phys. Chem. Ref. Data* 11, Sup. 2, 1–392. doi: 10.1063/1.555845
- ZEBEC, V. & RADANOVIĆ-GUŽVICA, B. (1992): Crystallographic Determination of Titanite from Smilevski Dol in Selečka Mountain, Macedonia.– *Geol. Croat.*, 45, 63–68.

*Manuscript received April 30, 2012*

*Revised manuscript accepted August 12, 2012*

*Available online October 30, 2012*